A Comparison of Zero Mean Strain Rotating Beam Fatigue Test Methods for Nitinol Wire

Dennis W. Norwich, P.E.
Memry Corporation, Bethel, CT USA

Introduction

Zero mean strain rotating beam fatigue testing has become the standard for comparing the fatigue properties of Nitinol wire. Most commercially available equipment consists of either a two chuck or a chuck and bushing system where the wire length and center-to-center axis distance determines the maximum strain on the wire. For the two chuck system, the samples are constrained at either end of the wire and both chucks are driven at the same speed. For the chuck and bushing system, the sample is constrained at one end in a chuck and rides freely in a bushing at the other end. These equivalent systems will both be herein referred to as chuck-to-chuck systems. An alternate system uses a machined test block with a specific radius to guide the wire at a known strain during testing. In either system the test parts can be immersed in a temperature controlled fluid bath to eliminate any heating effect created in the specimen due to dissipative processes during cyclic loading (cyclic stress induced formation of martensite) [1]. This study will compare the results of the same starting material tested with each system to determine if the test system differences affect the final results. The advantages and disadvantages of each system will be highlighted and compared. The factors compared will include ease of set up, operator skill level required, consistency of strain measurement, equipment test limits, and data recovery and analysis. Also, the effect of test speed on the test results for each system will be investigated.

Sample Preparation

All of the samples for this study were produced from one lot of 0.53 mm diameter amber oxide wire (Ti-55.8/55.9 wt%Ni) which was drawn to yield approximately 45% cold work on the final material. All of test samples were shape set straight using the same heat treatment process: tooling, time, temperature, and heat source [2]. After heat treatment, the parts were cleaned ultrasonically in an isopropyl alcohol (IPA) and water solution with no additional chemical processing or surface treatment.

Chuck–to-Chuck Method Set Up

The set up of the chuck-to-chuck method starts with the calculations for determining the bending radius to give the required strain. The radius to strain relationship is defined by $\varepsilon = \frac{r}{R}$ x 100% where ε= strain, r= radius of the wire, and R= radius of curvature to the neutral axis of the wire [3]. Next the wire length and chuck-to-chuck distance required to yield the desired strain are calculated. These calculations do not include the additional length of wire that is inserted into each chuck. The curvature of the wire will not be a full radius but rather the ellipse-like shape represented below in Figure 1 and defined by the simplified calculations shown in Figure 1. These calculations were developed by Clarke and Bates of Hunter Spring Company ca. 1940 [4]. An actual image of a sample ready for test is shown in Figure 2. These calculations will give the minimum radius of the wire constrained only at the chucks. This minimum radius occurs only at the apex of the ellipse-like shape. Therefore, the design strain precisely occurs only at the apex of the ellipse-like shape.

The Clarke and Bates calculations were developed for standard materials yet have been widely adopted for use with pseudoelastic materials. The model was not designed to simulate the pseudoelastic plateau effect. Additionally, for Nitinol in pseudoelastic bending, the neutral axis must shift toward the compressive side to balance the distribution of tensile and compressive stresses in the cross section [5]. Therefore for strains above 1% which approximately correspond to the start of the pseudoelastic upper plateau, the Clark and Bates calculations will be less precise than when used below 1% strain on the elastic modulus portion of the stress-strain curve. This small loss of precision due to the combined effects listed above has largely been ignored or treated as inconsequential by industry.
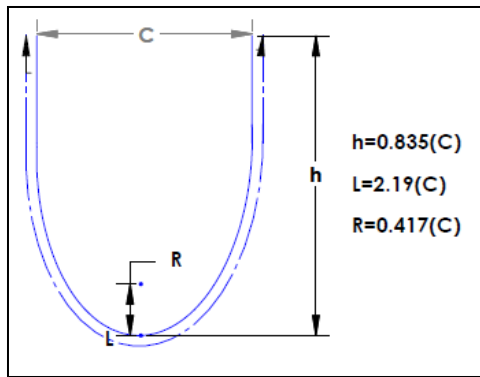
Figure 1: Chuck-to-Chuck Minimum Radius Calculations

Figure 2: Actual Sample Installed in Chucks

Machined Block Method Set Up

The set up of the machined block method starts with the calculations for determining the bending radius to give the required strain. The radius to strain relationship is defined by $\varepsilon = \frac{r}{R}$ x 100% where ε= strain, r= radius of the wire, and R= radius of curvature to the neutral axis of the wire [3]. Next a groove is machined into the polymer test block with a depth and width to provide sufficient clearance for the wire diamter being tested to reduce any effects of friction on the test sample [6]. A test block with with a specimen installed is shown below in Figure 3. A clear polymer cover is then installed on the block to retain the sample during test. The strain on the test sample is precisely the design strain calculated using the formula above for the enitre 90° of included arc length of the sample. A small marker is attached to the free end of the wire to register cycles to failure using a laser counting system.

As mentioned above, for Nitinol in pseudoelastic bending, the neutral axis must shift toward the compressive side to balance the distribution of tensile and compressive stresses in the cross section [5]. Therefore for strains above 1% which approximately correspond to the start of the pseudoelastic upper plateau, these simplified calculations for the uniform stress in this test method will also be less precise than when used below 1% strain on the elastic modulus portion of the stress-strain curve. This small loss of precision will be ignored for this research as this is the industry standard approach.
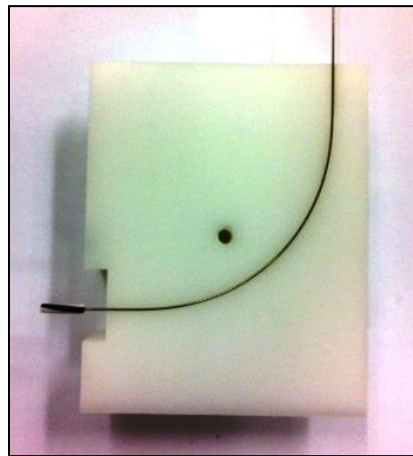

Figure 3: Test Sample in Machined Block

Chuck–to-Chuck Method Operation

For the style of chuck-to-chuck tester used in this research and shown below in Figure 4, chuck–to-chuck spacing and test speed are entered through the front panel. The style of break detection sensor on this machine consists of two brass plates on an adjustable arm as shown below in Figure 5. The plates are positioned so that the edge of the broken sample will contact both plates and send a signal to the controller to stop the test. The sample is immersed in the temperature controlled circulating water bath and run to failure or run out. This equipment can run one sample at a time at test speeds of 20 to 10,000 RPM
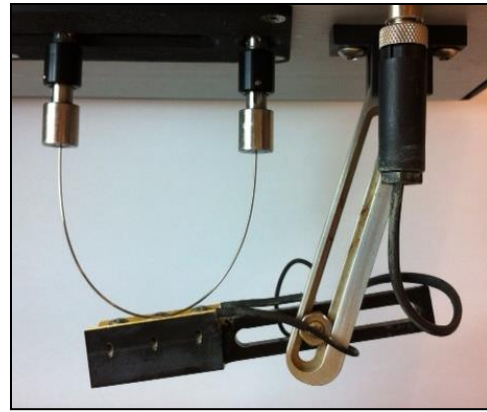
Figure 4: Complete System with Water Bath

Figure 5: Sample with Break Sensor in Place

Machined Block Method Operation

For the machined block tester used in this research and shown below in Figures 6 and 7, the strain is controlled by the test block used and the speed is set on a motor control. Break detection is accomplished by a laser counter sensing the rotation of the marker on the free end of the test sample. The sample is immersed in the temperature controlled circulating water bath and run to failure or run out. The equipment is manually stopped by the operator when all samples fail or run out is reached. This equipment can run ten samples at a time at test speeds of 100 to 1,500 RPM.
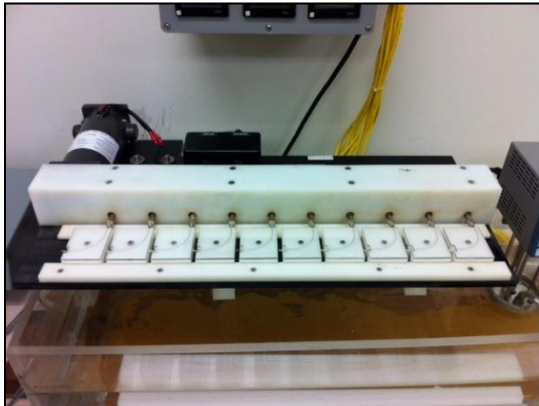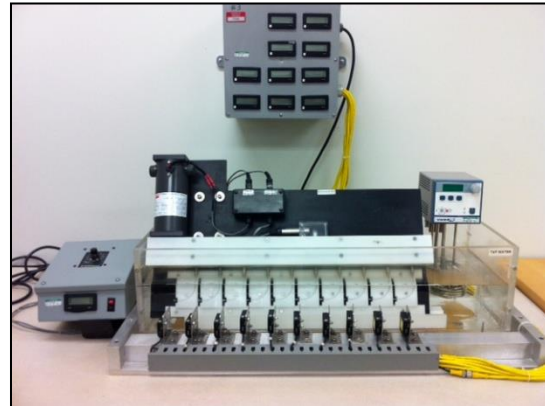

Figure 6: Samples Installed in Test Blocks

Figure 7: Complete System with Water Bath

Chuck–to-Chuck Method Data Recovery and Analysis

After test, the length of each wire section must be precisely measured. If the wire is broken at a spot other than the center of the test specimen as is shown in Figure 8, then the actual strain at the break must be calculated using a correction factor based on the location of the break. Table 1 below shows selected data from the correction factor table developed by Clarke and Bates of Hunter Spring Company ca. 1940 [4]. Sample calculations based on the formulas shown in Figure 1 are shown below. The wire measurements post fracture do not include the additional lengths of wire that are inserted into the chucks. Only the free unsupported lengths are included in these calculations.

Wire Diameter: 0.53 mm

Design Strain: 1.00%

$$R = \frac{r}{\varepsilon} = \frac{0.265}{0.01} = 26.5 \text{ mm}$$

$$C = \frac{R}{0.417} = \frac{26.5}{0.417} = 63.5 \text{mm}$$

L=2.19C=2.19(63.5)=139 mm

Post Fracture Length L1=60 mm

Post Fracture Length L2=79 mm

$$\% \text{ Difference} = \frac{(L2-L1)}{2L} \; x \; 100\% = \frac{(79-60)}{2(139)} \text{ x } 100\% = 6.8\% \text{ Difference}$$

Using Table 1 Below, Strain Correction Factor is Approximately 3.4%

Actual Strain at Break = 1.00(1-0.034) = 0.966%

Figure 8: Uneven Break Length

Table 1: Strain Correction Factor

Length Difference (%)	Strain Correction Factor (%)
1.0	0.1
2.0	0.3
3.0	0.7
4.0	1.2
5.0	1.7
6.0	2.5
7.0	3.4
8.0	4.4
9.0	5.6
10.0	6.7
15.0	14.4
20.0	24.3

Figures 9 and 10 below show SEM images of a sample after test. The sample fracture edges contact the break sensor to stop the test and register the cycles to failure. It takes a finite amount of time for the machine to register the break and come to a complete stop. In that time, the edge of tha facture suface gets slighly burninshed and rolled over. This can make detection of the fracture initiation point difficult. An alternate break detector shown in Figure 11 below contacts the wire away from the break edge and eliminates this problem.
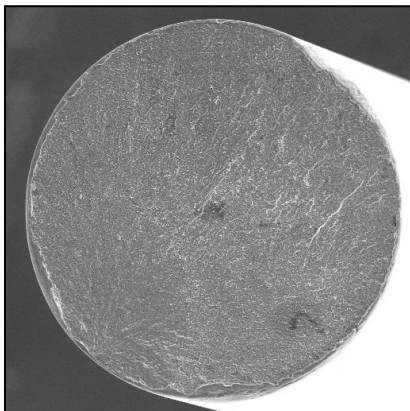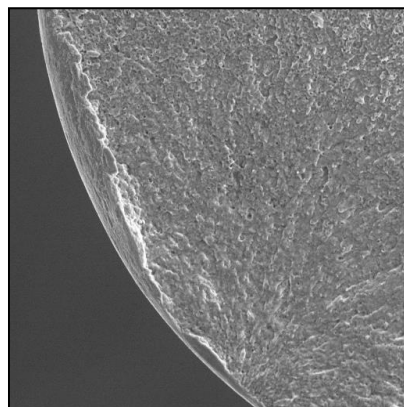
Figure 9: SEM Image of Fracture Surface

Figure 10: SEM Image of Burnished Edge

Figure 11: Alternate Break Sensor to Eliminate Edge Burnishing

Machined Block Method Data Recovery and Analysis

Any break within the 90° of included arc length will be precisely at the design strain [6]. The laser counter will stop counting as soon as it detects no motion in the marker attached to the free end of the wire. The remainder of the wire that is attached to the driving chuck will continue to rotate until the test is suspended. Because of this, it is possible to see multiple breaks in one length of wire as shown in Figure 13 below. Only the first break at the free end of the wire occurs at the recorded number of cycles to failure.
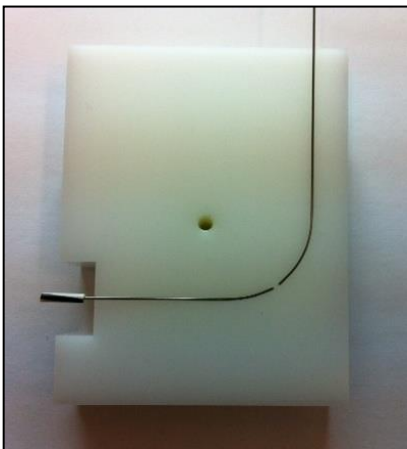
Figure 12: Typical Broken Sample
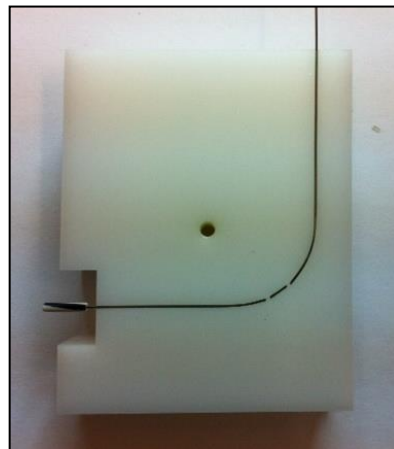
Figure 13: Sample with Multiple Breaks

Because of the energy stored in the strained wire, the pieces of the broken wire usually spring apart immediately upon fracture. However, a small number (approximately 5 to 10%) of the wire samples will remain close enough to rub face to face for several revolutions. This can lead to face burnishing of the fracture surface as shown in Figures 14 and 15 below. This burnishing can ruin any chance at fracture analysis but only occurs in a small percentage of the fractures.
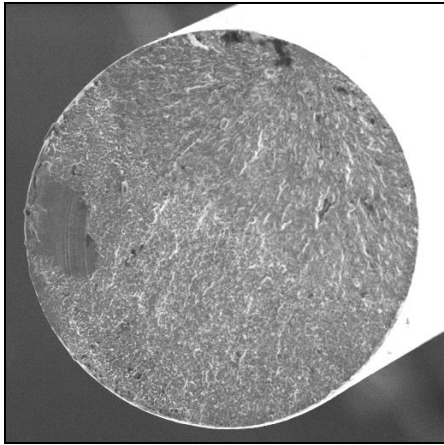
Figure 14: SEM Image of Fracture Surface
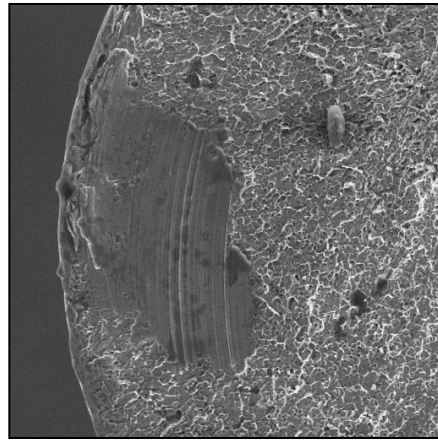
Figure 15: SEM Image of Burnished Face

Results

The results of the fatigue testing comparison are shown below. Table 2 includes all the individual data. Figures 16, 17, and 18 are plots of the average values. For the plots, each data point represents the average of five samples for each strain level and test condition. The data show very similar results for both test methods and all test speeds when tested at or below 1.0% strain. At strains above 1.0%, there is significantly greater variation in results.

The similar results at or below 1% strain demonstrate that the test methods can provide equivalent data. The water lubricated test blocks in the machined block method do not add significant friction to the test sample to affect the results. The soft polymer blocks do not polish the samples or smooth the sample surface during test. Therefore they do not artificially increase the resulting fatigue life.

For the individual test methods, below 2% strain, there was no difference in results based on test speed. This demonstrates that for each method the temperature controlled bath effectively eliminates any heating effect created in the specimen due to dissipative processes during cyclic loading (cyclic stress induced formation of martensite) [1]. This allows faster test speeds without compromising the results.

At 2.5% strain, which is the highest strain tested for this research, there is the most variation. As fatigue life is a stochastically controlled phenomenon, this is not unexpected. Experience shows that with more data points, the data will normalize even at 2.5% or higher strain.

As noted above, the Clark and Bates calculations are less precise for strains above 1%. They were modeled on standard materials without a pseudoelastic plateau. The slight deviation of actual stresses from the design conditions could contribute partially to the reduced fatigue life for the chuck-to-chuck method in the plateau region.

This single significant difference determined in this research is the increased fatigue life by the Machined Block method in the 1% to 2% strain region. At greater than 1% strain, the test sample is loaded on the pseudoelastic plateau. For the machined block method, the enitre 90° of included arc length of the sample is loaded precicely at the same plateau strain and is constrained from any vibration by the test block. For the chuck-to-chuck method, only the apex of the test sample will be at the design plateau strain. Because the sample is unrestrained, vibration can cause the high strain apex to "walk" along the test sample as the testing proceeds. This leads to a non-homogeneous stress induced martensite distribution and therefore a moving area of stress concentration [5]. See Figure 19 below for an image of a high strain sample loaded on the pseudoelastic plateau where the apex of the eliplse has "walked" off center. Even with an external vibaration damping device, the high strain apex can "walk" off center. This strain variation can lead to premature fatigue failure [7].
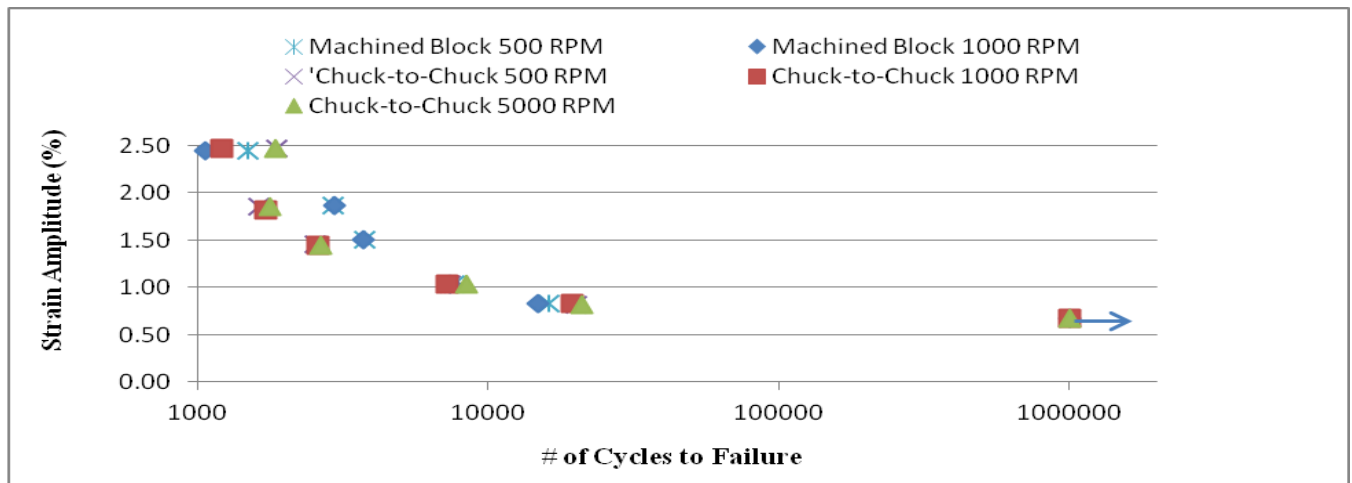
Table 2: Individual Fatigue Data

Test Method	Test Speed	Average Strain	Cycles to Fail Sample #1	Cycles to Fail Sample #2	Cycles to Fail Sample #3	Cycles to Fail Sample #4	Cycles to Fail Sample #5	Average Cycles to Fail	Population Standard Deviation
Machined Block	500	2.45	1221	2131	1500	1305	1293	1490	334
Machined Block	500	1.87	3054	3163	3067	2907	2511	2940	230
Machined Block	500	1.50	3779	3759	3747	3865	3588	3748	90
Machined Block	500	1.04	9051	7691	6731	7167	7459	7620	784
Machined Block	500	0.83	19318	14337	14891	16346	17279	16434	1779
Machined Block	500	0.68	1000000+	1000000+	1000000+	1000000+	1000000+	1000000+	n/a
Machined Block	1000	2.45	940	1110	1236	1035	1014	1067	100
Machined Block	1000	1.87	3020	2806	3396	2661	2973	2971	248
Machined Block	1000	1.50	3960	3837	3866	3571	3408	3728	206
Machined Block	1000	1.04	7950	5379	8695	6865	8048	7387	1164
Machined Block	1000	0.83	15815	15187	16476	14549	13330	15071	1081
Machined Block	1000	0.68	1000000+	1000000+	1000000+	1000000+	1000000+	1000000+	n/a
Chuck-to-Chuck	500	2.47	1565	1829	1905	2380	1657	1867	283
Chuck-to-Chuck	500	1.85	1434	1752	2178	1616	1154	1627	341
Chuck-to-Chuck	500	1.45	2846	2716	2397	2673	2133	2553	256
Chuck-to-Chuck	500	1.03	7265	7730	7253	7064	7590	7380	243
Chuck-to-Chuck	500	0.82	21891	23189	21591	16759	16801	20046	2720
Chuck-to-Chuck	500	0.67	1000000+	1000000+	1000000+	1000000+	1000000+	1000000+	n/a
Chuck-to-Chuck	1000	2.47	1118	1331	1179	1100	1334	1212	102
Chuck-to-Chuck	1000	1.82	1977	1637	1287	2278	1413	1718	365
Chuck-to-Chuck	1000	1.45	2701	2484	2928	2448	2467	2606	185
Chuck-to-Chuck	1000	1.04	7620	8028	6939	6953	6715	7251	493
Chuck-to-Chuck	1000	0.83	22119	16298	18856	20371	19676	19464	1914
Chuck-to-Chuck	1000	0.67	1000000+	1000000+	1000000+	1000000+	1000000+	1000000+	n/a
Chuck-to-Chuck	5000	2.47	2289	1991	1587	1758	1626	1850	261
Chuck-to-Chuck	5000	1.85	1614	2101	1168	2525	1510	1784	476
Chuck-to-Chuck	5000	1.45	2163	2956	2683	3136	2349	2657	363
Chuck-to-Chuck	5000	1.03	8476	8641	8493	8497	8189	8459	148
Chuck-to-Chuck	5000	0.82	20729	20479	21069	21256	21517	21010	369
Chuck-to-Chuck	5000	0.67	1000000+	1000000+	1000000+	1000000+	1000000+	1000000+	n/a

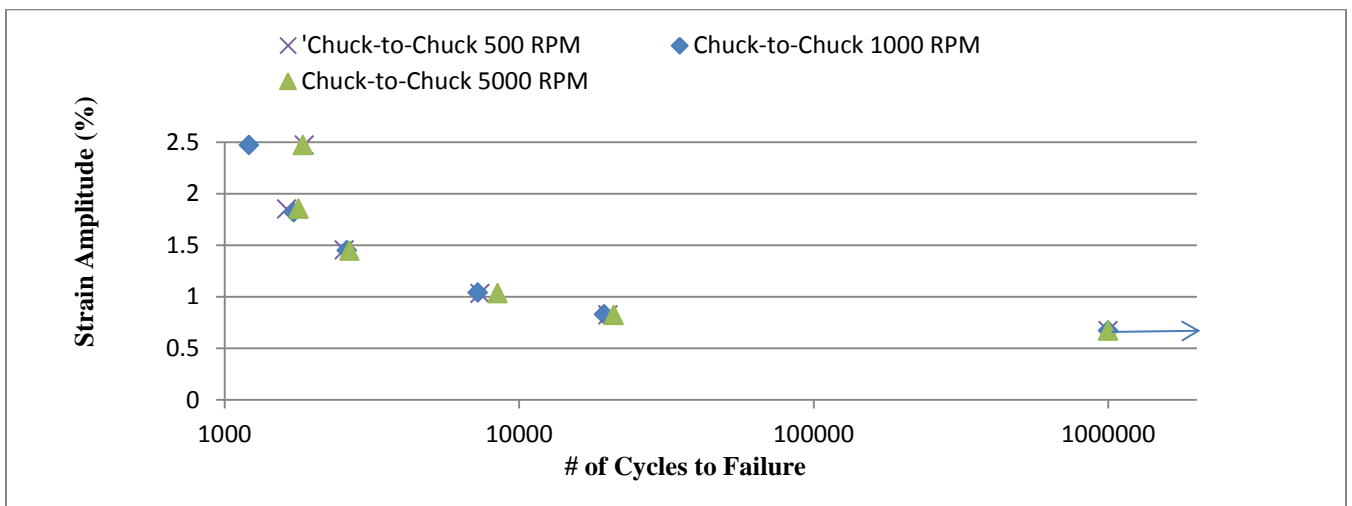*Figure 16: Fatigue Testing Results Complete ε-N Curve*

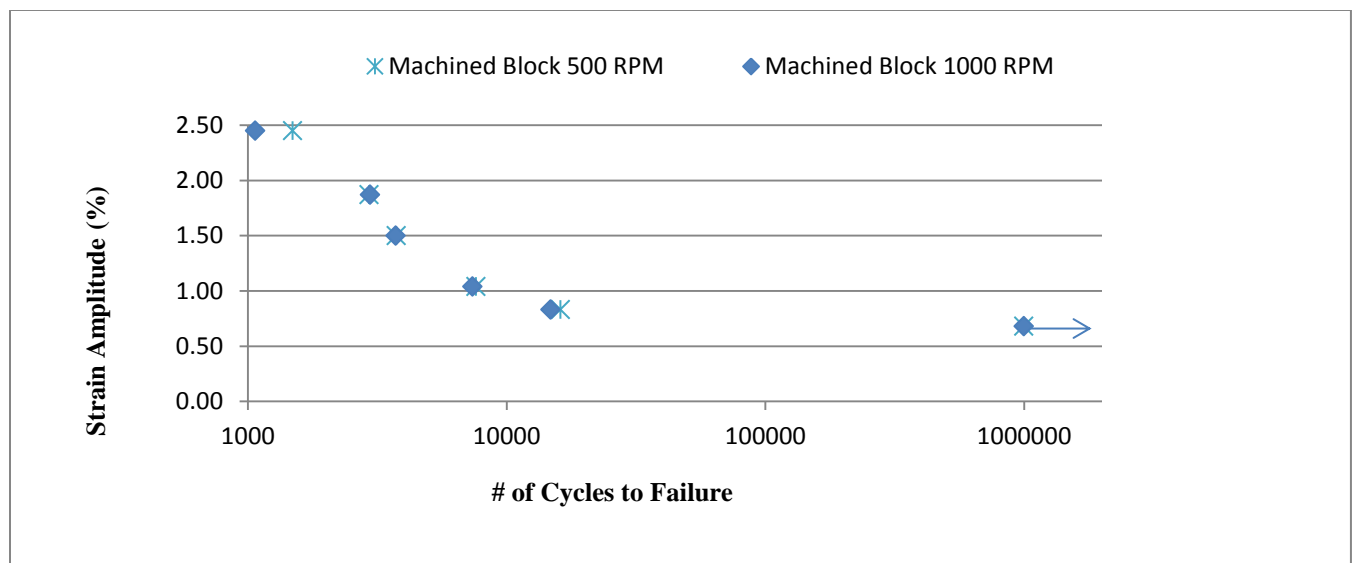*Figure 17: Fatigue Testing Results Chuck-to-Chuck ε-N Curve*

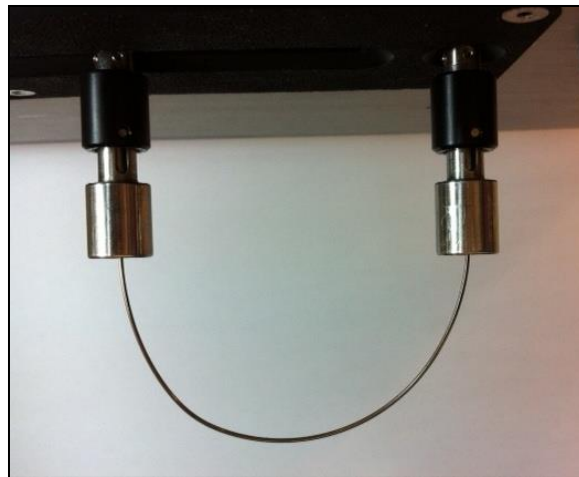*Figure 18: Fatigue Testing Results Machined Block ε-N Curve*

Figure 19: Uneven Strain on Superelastic Plateau

Summary

Each of the fatigue test methods evaluated here have advantages and disadvantages. The chuck-to-chuck method requires no hard tooling and can be run at very high speeds but precise strain measurement and consistency at high strain can be problematic. The machined block method can test 10 samples at a time with very precise strain control but is limited in test speed and requires machined tooling for each diameter/strain combination. Table 3 below summarizes the advantage and disadvantages of the two methods.

The decision on which method is best is dependent on the application. For example, for high speed testing with a variety of wire diameters and strain levels, the chuck-to-chuck method offers the most flexibility and does not require manufacture of hard tooling and therefore is the obvious choice. A typical application would be screening large numbers of variables to determine their effect on fatigue life.

However, for testing large numbers of samples at the same diameter/strain level or for applications where the precise strain at fracture must be controlled, the machined block method is clearly superior. A typical application would be a pass/fail quality requirement where 100 samples must exceed 10,000 cycles at 1.2% strain for acceptance of a wire lot.

Table 3: Comparison Table of the Two Methods

Parameter	Chuck-to-Chuck	Machined Block
Normal Operating Speed (RPM)	1000	1000
Minimum Operating Speed (RPM)	20	100
Maximum Operating Speed (RPM)	10,000	1500
Tooling	None	Blocks
Ease of Sample Preparation	Medium	Easy
Minimum Strain for ø0.53 mm Sample (%)	0.57	0.45
Maximum Strain for ø0.53 mm Sample (%)	2.90	6.00
Wire Length at Minimum Strain (mm)	260	125
Wire Length at Maximum Strain (mm)	72	125
Integrity of Broken Sample	High	Medium
Ease of Data Recovery	Medium	Easy
Potential for Vibration	High	Low
Potential for Strain Inconsistency	High	Low
Maximum Number of Samples per Run	1	10

References

[1] M. Wagner, T. Sawaguchi, G. Kaustrater, D. Hoffken, G. Eggeler, "Structural Fatigue of Pseudoelastic NiTi Shape Memory Wires", Materials Science and Engineering A 378, (2004) p. 105- 109.

[2] A. Pelton, J. DiCello, S. Miyazaki, "Optimization of Processing and Properties of Medical-Grade Nitinol Wire", SMST-2000 Proceedings of the International Conference on Shape Memory and Superelastic Technologies eds S.M. Russel and Alan R. Pelton, (Pacific Grove, California: International Organization on SMST, 2001) p.361-374.

[3] D. Norwich, A. Fasching, "A Study on the Effect of Diameter on the Fatigue Properties of NiTi Wire", SMST-2008 Proceedings of the International Conference on Shape Memory and Superelastic Technologies, eds A. Tuissi, M. Mitchell, J. San Juan (Stresa, Italy, 2009) p. 558-562.

[4] P. C. Clarke, A. C. Bates, Hunter Spring Company ca. 1940.

[5] B. Reedlunn, C. Churchill, E. Nelson, J. Shaw, S. Daly, "Tension, Compression, and Bending of Superelastic Shape Memory Tubes", Journal of the Mechanics and Physics of Solids, Volume 63, February 2014, p. 506-537.

[6] M. Polinsky, D. Norwich, M. Wu, "A Study on the Effects of Surface Modifications and Processing on the Fatigue Properties of NiTi Wire", SMST-2006 Proceedings of the International Conference on Shape Memory and Superelastic Technologies, eds B. Berg, M. Mitchell, J. Proft (Pacific Grove, CA, 2008) p. 1-17.

[7] Z. Lin, K. Pike, M. Schlun, A. Zipse, J. Draper, "Nitinol Fatigue Life for Variable Strain Amplitude Fatigue", SMST-2011 Proceedings of the International Conference on Shape Memory and Superelastic Technologies, ed M. Mitchell, (Hong Kong, China, 2012) p. 2628-2632.